Published in final edited form as:
Biomaterials. 2008 October ; 29(30): 4082–4090. doi:10.1016/j.biomaterials.2008.06.027.

Multilayer Nanofilms as Substrates for Hepatocellular Applications

Corinne R. Wittmer[a], **Jennifer A. Phelps**[a], **Christin M. Lepus**[b], **W. Mark Saltzman**[c], **Martha J. Harding**[b], and **Paul R. Van Tassel**[a,*]

a*Department of Chemical Engineering, Yale University, New Haven, CT 06520-8286, USA*

b*Section of Comparative Medicine, Yale University School of Medicine, New Haven, CT 06520-8016 USA*

c*Department of Biomedical Engineering, Yale University, New Haven, CT 06520-8260, USA*

Abstract

Multilayer nanofilms, formed by the layer-by-layer (LbL) adsorption of positively and negatively charged polyelectrolytes, are promising substrates for tissue engineering. We investigate here the attachmemt and function of hepatic cells on multilayer films in terms of film composition, terminal layer, rigidity, charge, and presence of biofunctional species. Human hepatocellular carcinoma cells (HepG2), adult rat hepatocytes (ARH), and human fetal hepatoblasts (HFHb) are studied on films composed of the polysaccharides chitosan (CHI) and alginate (ALG), the polypeptides poly(L-lysine) (PLL) and poly(L-glutamic acid) (PGA), and the synthetic polymers poly(allylamine hydrochloride) (PAH) and poly(styrene sulfonate) (PSS). The influence of chemical cross-linking following LbL assembly is also investigated. We find HepG2 to reach confluence after seven days of culture on only 2 of 18 candidate multilayer systems: $(PAH\text{-}PSS)_n$ (i.e. n PAH-PSS bilayers) and cross-linked $(PLL\text{-}ALG)_n$-PLL. These two systems, as well as cross-linked $(PLL\text{-}PGA)_n$-PLL, support attachment and function (in terms of albumin production) of ARH, provided collagen is adsorbed to the top of the film. $(PAH\text{-}PSS)_n$, cross-linked $(PLL\text{-}ALG)_n$, and cross-linked $(PLL\text{-}PGA)_n$-PLL films all support attachment, layer confluence, and function of HFHb, with the latter film promoting the greatest level of function at 8 days. Overall, film composition, terminal layer, and rigidity are key variables in promoting attachment and function of hepatic cells, while film charge and biofunctionality are somewhat less important. These studies reveal optimal candidate multilayer biomaterials for human liver tissue engineering applications.

Keywords

layer-by-layer; multilayer film; nanofilm biomaterial; hepatocyte; liver

1. Introduction

Each year, end-stage liver disease claims thousands of lives in the US [1]. Orthotopic liver transplant is currently the only treatment for end-stage liver disease, but is far from ideal owing to its high cost, the adverse effects associated with surgery and immuno-suppression, and the severe lack of donor organs. Liver tissue engineering, where one seeks to augment liver

*Corresponding author at paul.vantassel@yale.edu.

function by implanting functional hepatocytes, offers an attractive alternative [1–6]. Important challenges include the large number of cells necessary for clinical benefit (at least 10% of the native liver mass) and the need to provide a suitable environment for their long-term engraftment. A promising strategy is to create functional cellular constructs within an implantable biomaterial support device, such as a porous polymer scaffold. Optimal device design may allow for enhanced initial number, survival, growth, and function of transplanted cells, but a key challenge is to optimize the cell-biomaterial interactions, so that transplanted cell survival and function is maximized.

Biomaterials comprising tissue engineering support devices must exhibit appropriate chemical, mechanical, and biofunctional properties to allow cells to efficiently attach, proliferate, and function. Previous work focusing mainly on rodent systems has shown adult hepatocytes to attach, proliferate (to a limited extent), and form flat structures, but exhibit limited function, on mechanically rigid materials and/or materials containing adhesion promoting ligands, and to function and be more rounded, but not proliferate, on mechanically compliant materials and/or materials with fewer adhesion-promoting ligands [7–9]. Biofunctional and mechanical influences may even be used together to control morphology and functional fate, but attachment/proliferation and function are typically inversely related [10–12]. Less is known of substrate influence on human hepatocytes and their progenitors. Because adult human hepatocytes are not routinely available and generally exhibit very limited proliferation *in vitro*, human hepatic progenitor cells, as found among cells isolated from the fetal liver, represent a promising cell source. While recent studies utilizing rodent [13–16] and human [17–19] hepatocyte progenitors testify to their significant proliferative capacity, the focus has generally been on controlling differentiation *in vitro* through soluble cytokines and growth factors rather than on their biomaterial interactions.

Multilayer nanofilms, formed by the layer-by-layer (LbL) method, are promising biomaterials for a variety of cell contacting applications owing to their ease of formation and the possibility to tailor their chemical, mechanical, and biofunctional (i.e. via immobilized biomolecules) properties [20–33]. LbL assembly occurs through the alternate adsorption of positively and negatively charged polyelectrolytes, and the resultant multilayer films can be rendered bioactive through the adsorption of protein or other biological molecules capable of transmitting signals to contacting cells. The mechanical properties of the film – e.g. stiffness, hydration, density, thickness – can be controlled very precisely by the choice of polymer, solution conditions (pH and ionic strength), post-formation chemical cross-linking steps, and number of layers. Hepatocytes tend to be sensitive to substrate properties [7–12], and thus appear to be well-suited targets for modulation by LbL assembled multilayer films. However, little is currently known [25,33].

In this work, we investigate the attachment, growth, viability, and function of three hepatocellular systems cultured on multilayer film biomaterials: 1) human hepatocellular carcinoma (HepG2) cells, convenient owing to their ease of handling, indefinite proliferation, and weak anchorage dependence, 2) adult rat hepatocytes (ARH), thought to be an acceptable analog to human cells, and 3) human fetal hepatoblasts (HFHb), progenitor cells capable of significant proliferation. We consider multilayer films composed of polypeptides, polysaccharides, and/or synthetic polymers – each chosen based on previous success in other cell contacting applications. We investigate the influence of film composition, post-formation chemical cross-linking, and the presence of extra-cellular matrix protein terminal layers. We characterize multilayer films via optical waveguide lightmode spectroscopy (OWLS) and quartz crystal microgravimetry with dissipation (QCMD), and analyze cell attachment/viability/growth via optical microscopy and cell function in terms of albumin secretion. We seek to understand the influence of film chemical, mechanical, and biofunctional properties on

the behavior of hepatocellular systems, and to determine best candidate materials for eventual human liver tissue engineering applications.

2. Materials and Methods

2.1. Optical Waveguide Lightmode Spectroscopy (OWLS)

OWLS is a very precise (to about 1 ng/cm^2) optical detection method for measuring macromolecular adsorption at the solid-liquid interface [34–37]. The sensing principle involves the excitation of guided modes via a polarized laser beam directed upon a grating coupler at the surface of an optical waveguide. The mass and thickness of an adsorbed layer can be related to changes in the guided modes through an optical model, such as one assuming an optically uniform adsorbed layer [38]. Our OWLS instrument (OWLS 110, MicroVacuum, Budapest) is composed of a parallel plate flow cell whose bottom surface is an OW 2400 Sensor Chip (MicroVacuum), consisting of a planar $Si_{1-x}Ti_xO_2$ waveguide (x=0.25±0.05) coated onto a glass substrate.

2.2. Quartz Crystal Microgravimetry with Dissipation (QCMD)

A QCM consists of a thin quartz disc sandwiched between a pair of electrodes. The resonant frequency of the crystal, when excited by an AC voltage, depends on the total oscillating mass, including coupled water. A “soft” (viscoelastic) adsorbed layer will dampen the crystal's oscillation [39–42]. The dissipation may be measured at multiple frequencies and by applying a viscoelastic model, the mass, thickness, elastic shear modulus, and shear viscosity of the adhering film can be determined. Our QCMD instrument (D300, Q-Sense, Sweden) is composed of a parallel plate flow cell whose bottom surface is a QSX 303 Sensor Chip (Q-Sense), consisting of a planar SiO_2 coating on a quartz crystal.

2.3. Multilayer film formation/protein adsorption

Reagents—Low viscosity alginate (ALG), poly(L-lysine) (PLL; 70–150 kDa), poly(L-glutamic acid) (PGA; 3–15 kDa), poly(sodium 4-styrene sulfate) (PSS; 70 kDa), rat collagen type I (rCI), human collagen types IV (hCIV), poly(allylamine hydrochloride) (PAH; 15 kDa), low molecular weight chitosan (CHI), lactobionic acid (LA) and sulfo-NHS are obtained from Sigma; NHS and EDC from Fischer Scientific (Suwance, GA); and human collagen type I (hCI) from VWR international (Bridgeport, NJ). The buffer solution is 10 mM Bis-Tris with 150 mM NaCl adjusted at pH 6 with acetic acid. The polymer concentrations are 0.4 g/L for PLL and PGA, 0.5 g/L for CHI, ALG, PSS and PAH, and 0.1 mg/ml for Galactosylated Chitosan (GALCHI). All polymer solutions (polymer plus buffer) are adjusted to pH 6. All polymers are used as received except for the galactosylated chitosan, which is made using the protocol of Chung, et al [43]. rCI and hCIV (hCI) are dissolved in acetic acid at concentration 0.1 mol/L (0.5 mol/L) and then diluted in Bis-Tris buffer to their final concentration.

Chemical cross-linking—Cross-linking is performed on films built either on 24-well plates or $SiTiO_2$ sensor ships. The cross–linking solution is a mixture of EDC at 400 mM and sulfo-NHS at 100 mM in a 10 mM Bis-Tris buffer with 150 mM NaCl adjusted at pH 5.5. Multilayer films are soaked in a fresh cross-linking solution for 16 hours. Films grown in the OWLS system are rinsed with Bis-Tris buffer under flow (volumetric flow rate 80 μL/min), while those formed in culture wells are rinsed 3 times for an hour. The protocol successfully tested by Richert, et al [44] is followed, except that Bis-Tris buffer is used and four additional hours of exposure to the cross-linking solution are employed.

Multilayer films in 24 well plates—Standard 24 well polystyrene plates are employed. A polymer solution is introduced into a well and maintained for 15 min, during which time an adsorbed polymer layer forms. A solution of pure buffer then replaces the polymer solution,

and is maintained 8 min (this step is repeated once). Each subsequent layer is introduced by a 15 min adsorption step and 2 rinsing steps of 8 min. For cross-linked films, an EDC/sulfo-NHS solution is introduced for 16 hours and then rinsed 3 times with the Bis-Tris buffer for 1 hour. In certain cases, a layer of collagen is adsorbed for 30 min and rinsed 15 min with Bis-Tris and 3 times with PBS for 1 hour. Each experiment is duplicated.

Multilayer films with OWLS/QCMD—To avoid bubble formation, the buffer is degassed in an ultrasonic bath for 25 min prior to use. A sensor chip is washed with 2% Hellmanex (Hellma, Mulheim, Germany), a commercial glassware detergent. The sensor chip is then rinsed with deionized water and placed in the flow cell. A buffer solution is continuously introduced into the flow cell, at a flow rate of 80 μL/min, until a stable baseline is achieved. A solution of polymer is then introduced for 15 min, and a buffer rinse of 15 min follows. Each subsequent layer is introduced by a 15 min adsorption step and a 15 min rinsing step. For cross-linked film, the EDC/sulfo-NHS solution is introduced for 20 min under flow condition, and then the flow is stopped for 16 hours. The EDC/sulfo-NHS solution is then rinsed with the Bis-Tris buffer for one hour and a layer of collagen is adsorbed for 30 min and rinsed. For certain films, a layer of collagen is adsorbed for 30 min and rinsed until desorption becomes negligible.

2.4. Cell culture

Human hepatocellular carcinoma cells (HepG2) are cultured in Minimum Essential Medium Eagle (ATCC, Manassas, VA) plus 1% penicillin / streptomycin (Sigma, St. Louis, MO) and 10% fetal bovine serum (Sigma). Half of the medium is changed every 2 days. Cells are cultured in a 75 cm^2 flask until they reach 70% confluence, detached from the flask with 0.5 g/L trypsin and 0.2 g/L EDTA and seeded on 24-well polystyrene plates coated with multilayer films at a concentration of 2.5×10^4 cells/cm^2. The polystyrene well without multilayer film serves as the control.

Suspensions of adult Sprague-Dawley rat hepatocytes (ARH) are harvested in the Yale University Cell Isolation Core Facility using an established 2-step collagenase protocol as previously described [45]. Cells are immediately seeded on 24-well plates coated with multilayer films at a concentration of 2.5×10^4 cells/cm^2 in William's Medium E (Sigma) supplemented with HEPES (10 mmol/L; Invitrogen, Carlsbad, CA) glutamine (2 mmol/L; Invitrogen); dextrose (1.8 mg/L; Sigma), gentamycin (8 mg/L; Invitrogen), dexamethasone (1 μmol/L), ITS supplement (4 mg/L; Sigma), 5% Fetal Bovine Serum (Sigma), and an antibiotic-antimycotic composed of 200 units/mL penicillin, 200 mg/L streptomycin, and 0.5 mg/L amphotericin B (Invitrogen). 70% of the medium is changed daily. A rat collagen type I coated tissue culture plate (Biocoat, BD Biosciences, San Jose, CA) serves as the control.

Following all institutional approvals and with the mother's consent, human fetal liver tissue is harvested following an elective termination from a 16 week-old gestational age abortus, by staff of the Human Fetal Tissue Repository, Albert Einstein College of Medicine, NY. Human fetal hepatoblasts (HFHb), along with associated stromal cells, are harvested by digesting liver tissue with 5 g/L collagenase type D (Roche, Indianapolis IN) at 37°C for 30 minutes with gentle agitation. Harvested cells are allowed to attach to plates in William's E medium supplemented with nicotinamide (10 mmol/L); HEPES (20 mmol/L); $NaHCO_3$ (17 mmol/L); pyruvate (550 mg/L); ascorbic acid-2-phosphate (0.2 mmol/L); glutamine (2mmol/L); dexamethasone (10^{-7} mol/L); ITS+ premix containing insulin (6.25 g/L), transferrin (6.25 g/L) and selenious acid (6.25 μg/L); bovine serum albumin (1.25 g/L); linoleic acid (5.35 μg/L); 5% fetal bovine serum, an antibiotic-antimycotic composed of 200 units/mL penicillin, 200 mg/L streptomycin, 10 mg/L gentamycin, and 0.5 mg/L amphotericin B (Invitrogen) [17]. After 4 hours, the medium is changed to remove serum and epidermal growth factor is added (20 μg/L). All cultures are maintained at 37°C in a 5% CO_2 incubator with half of the medium

changed every 2 days. To expand cell numbers, the cultures are passaged twice, using a 2-step EGTA (Sigma) and then collagenase (type IV) dispase (Roche, Indianapolis, IN) treatment [17] and seeded on 24-well plates coated with multilayer films at density of 1.25×10^5 cells/cm^2. A rat collagen type I coated tissue culture plate (Biocoat, BD Biosciences, San Jose, CA) serves as the control.

2.5. Cell attachment / growth

Cell attachment and growth is assayed via images obtained from a phase contrast optical microscope (IX71, Olympus, Center Valley, PA).

2.6. Albumin secretion

The quantity of albumin released by cells into the medium is determined by indirect sandwich enzyme-linked immunosorbent assay (ELISA). Rat and human albumin ELISA quantification kits are from Bethyl Laboratories, Inc (Montgomery, TX).

3. Results

3.1. Human hepatocellular carcinoma (HepG2) cells

We begin by investigating the attachment and growth of HepG2 cells on a number of multilayer films. As polyelectrolyte building blocks, we consider the polysaccharides chitosan (CHI), galactosylated chitosan (galCHI), and alginate (ALG); the polypeptides poly(L-lysine) (PLL) and poly(L-glutamic acid) (PGA); and the purely synthetic polymers poly(allylamine) (PAH) and poly(styrene sulfonate) (PSS). In certain cases, we consider the influence of a chemical cross-linking step following LbL assembly. We employ the notation $(A\text{-}B)_n$ to indicate a film formed from n A–B bilayers, and $(A\text{–}B)_n$-A to indicate a films formed by n A–B bilayers plus one additional layer of A.

We seed cells initially at ~20% coverage, and then measure percent coverage at 3 and 7 days (Table 1 and Figure 1). In the case of the polysaccharide films $(CHI\text{-}ALG)_4$, $(CHI\text{-}ALG)_3$-CHI, $(galCHI\text{-}ALG)_4$, $(galCHI\text{-}ALG)_3$-galCHI, $(CHI\text{-}ALG)_4$-X, $(CHI\text{-}ALG)_3$-CHI-X, $(galCHI\text{-}ALG)_4$-X, $(galCHI\text{-}ALG)_3$-galCHI-X (X indicating a cross-linking step), and the polypeptide-polysaccharide films $(CHI\text{-}PGA)_4$, $(CHI\text{-}PGA)_3$-CHI, (CHI-PGA)-X, and $(CHI\text{-}PGA)_3$-CHI-X, we observe no appreciable cell attachment. Attachment and growth is more pronounced on one polypeptide-polysaccharide pair, PLL-ALG. We observe a few cells on $(PLL\text{-}ALG)_4$ after 7 days, 90% coverage on $(PLL\text{-}ALG)_3$-PLL after 5 days (data not shown; most cells detached after seven days) and 100% coverage (i.e. full confluence) on $(PLL\text{-}ALG)_3$-PLL-X after 7 days. For the synthetic polymer system, we observe full confluence on $(PAH\text{-}PSS)_4$ after 7 days, but only 80% coverage on $(PAH\text{-}PSS)_3$-PAH after 3 days and significant detachment after 7 days. As a control, we seed cells on a bare tissue culture plate and observe about 40% coverage after 3 days and full confluence after 7 days. Thus, of all the systems considered, we observe confluent HepG2 layers to form only on tissue culture polystyrene and on the $(PLL\text{-}ALG)_3$-PLL-X and $(PAH\text{-}PSS)_4$ films.

3.2. Adult rat hepatocytes (ARH)

We next investigate the attachment and growth of ARH on multilayer film biomaterials. We consider the PAH-PSS and PLL-ALG systems based on our HepG2 results, and the PLL-PGA system owing to its previously demonstrated cyto-compatibility [20]. We additionally consider the influence of the extracellular matrix protein rat collagen I (rCI).

In Table 2, we show the ARH percent coverage after 1 and 3 days in culture. While many systems show significant attachment at day 1, none exhibit any growth in cell number between days 1 and 3. In the absence of rCI, only the $(PAH\text{-}PSS)_5$ system supports non-negligible

coverage at day 3; $(PLL\text{-}PGA)_5$-X and $(PLL\text{-}PGA)_4$-PLL-X support ~50% coverage at day 1, but no cells are apparent at day 3. In contrast, all of the systems support at least 20% coverage in the presence of rCI. The PLL-ALG and PLL-PGA systems (with rCI) perform about as well as the rCI control, and generally outperform the PAH-PSS systems, in terms of ARH coverage. We observe no appreciable correlation between ARH coverage and the amount of adsorbed collagen (discussed in Section 3.4).

In Fig. 2, we show the albumin secretion of ARH after 2 and 4 days, as measured by ELISA. We observe only the rCI control layer to exhibit enhanced albumin secretion following 2 days (~ 1200 ng/mL/day), and all systems to be roughly equivalent after 4 days.

3.3. Human fetal hepatoblasts (HFHb)

We next investigate the attachment, growth, and function of HFHb on film compositions identical to those employed in the ARH studies. In addition, we consider films with a terminal layer of human collagen IV (hCIV), a prominent extra-cellular matrix protein within the human liver parenchyma. In many systems, fully or nearly confluent monolayers are achieved at day 1, reflecting strong attachment (Table 3). For the synthetic $(PAH\text{-}PSS)_5$ system, we observe the maintenance of a fully confluent layer throughout the 8 day period, irrespective of the presence of collagen. Only negligible attachment is observed on the $(PAH\text{-}PSS)_5$-PAH system without collagen. In the presence of rCI or hCIV, modest initial attachment is observed at day 1, and nearly confluent layers are present at day 4, reflecting growth among attached cells. However, neither of these systems supports confluence up to 8 days.

We also observe fully confluent layers at each time point, in the presence and absence of collagen, for the cross-linked polysaccharide-polypeptide $(PLL\text{-}ALG)_5$ system. Fully confluent layers are also observed at day 8 for the corresponding PLL terminated film; however, fewer cells are present at shorter time periods.

For the cross-linked polypeptide $(PLL\text{-}PGA)_5$ system, we observe strong (very strong in the presence of collagen) initial attachment, and nearly confluent layers at day 4. However, we observe confluence to be maintained for 8 days only in the presence of hCIV. In contrast, for the cross-linked $(PLL\text{-}PGA)_5$-PLL system, we observe strong initial attachment, and fully confluent layers at days 4 and 8, irrespective of the presence of collagen. Although confluence is reached at day 8 on the control plate (Biocoat plate with rCI), it is important to note that most of the systems considered here support higher levels of attachment at the time of seeding compared to the control.

We next consider the albumin secretion of the confluent systems described above. All systems considered produce albumin, indicating the presence of functional hepatoblasts and/or hepatocytes. In Fig. 3a, we consider films for which confluence is reached in the absence of collagen, and observe film composition to significantly influence the rate of albumin secretion. For $(PLL\text{-}PGA)_4$-PLL-X, the rate of albumin secretion is relatively high (~150 ng/mL) on days 1 and 3, but then steadily decreases over the next 5 days. For $(PLL\text{-}ALG)_5$-X, the albumin production peaks at day 5 and for $(PAH\text{-}PSS)_5$, the production steadily increases over 8 days.

We find the presence of collagen to have no measurable influence on the albumin secretion for the $(PAH\text{-}PSS)_5$ film (Fig. 3b). In contrast, albumin production in the $(PLL\text{-}PGA)_4$-PLL-X and $(PLL\text{-}ALG)_5$-X systems shows a marked collagen influence (Figs. 3c and 3d). In the former system, albumin secretion starts high (low) and steadily decreases (increases) in the absence (presence) of collagen, and in the latter system, the day 8 albumin secretion rate in the presence of rCI and hCIV is considerable greater than that of the collagen-free system. Only the $(PLL\text{-}PGA)_4$-PLL-X-rCI system meets the day 8 albumin production of the rCI control, and therefore may be the best overall candidate in terms of promoting liver cell function.

3.4. Multilayer films

In this section, we consider the physicochemical and protein adsorption characteristics of the PAH-PSS, PLL-ALG, and PLL-PGA multilayer films. In Fig. 4, we show film mass and thickness during LbL assembly, as measured via OWLS. We observe the mass and thickness of PAH-PSS to increase roughly linearly with layer number, while those of PLL-ALG and PLL-PGA to increase in a super-linear fashion. These results may be understood in the context of previous work identifying two LbL archetype assembly modes, linear and exponential, with the principal difference being discrete layering in the former case and a uniformly mixed film in the latter case [20,23].

We observe PAH-PSS films to be about three times as dense as the PLL-ALG and PLL-PGA films, based on film mass per area divided by the thickness (Table 4). We attribute this difference to the relatively low degree of hydration of the PAH-PSS system. We observe cross-linking to result in thinner, denser (and thus less hydrated) films.

We also show in Table 4 the mass of hCI and hCIV adsorbed on each of the polymer films. We observe the PSS-PAH system to be the most adsorbent for both proteins, and both cross-linked systems to adsorb significantly less protein. Among the cross-linked systems, films terminating in PLL exhibit a lower protein adsorption. PSS is known to be attractive to proteins; we find enhanced adsorption of hCIV but not hCI on the PSS terminated film. It is interesting to note the relatively high collagen adsorption to the $(PAH\text{-}PSS)_5$ system, for which liver cell attachment, proliferation, and albumin production is fairly collagen insensitive.

In Fig. 5, we show the shear modus, viscosity, and film thickness, as measured by QCMD, during film formation and following chemical cross-linking. The QCMD film thickness data qualitatively follow those obtained using OWLS. However, the former tend to be larger in magnitude, most likely due to the greater extent to which QCMD accounts for the presence of water trapped within the film interior. The increase in film thickness during cross-linking observed via QCMD (but not OWLS) is difficult to reconcile; although a decrease in overall film hydration is expected, perhaps some additional water is trapped near to the film surface owing to a decrease in the number of polymer loops and tails extending away from the interface. We find PLL-PGA and PLL-ALG films to have higher shear and viscous moduli compared to the PAH-PSS film, despite the higher mass/volume (Table 4) of the latter system. As expected, we find chemical cross-linking to increase film rigidity.

4. Discussion

Tissue engineering, where one seeks cellular constructs capable of providing functional support for diseased or damaged tissues, can benefit from biomaterials that promote cell attachment, proliferation, and function. Multilayer nanofilms formed via LbL assembly are promising in this regard owing to their ease of formation and the possibility to tailor their chemical, mechanical, and biofunctional properties. The human liver represents a challenging but important tissue system upon which biomaterial-based regenerative strategies can be developed. While many studies attest to the utility of LbL assembled films in cell-contacting applications, little is known about their application to hepatocellular systems. Our intention here is to take the first steps toward multilayer nanofilm-based tissue engineering of the human liver.

We construct multilayer film biomaterials employing polysaccharides, polypeptides, and purely synthetic species proven to be successful in previous cell-contacting applications. As polysaccharides, chitosan (CHI), alginate (ALG), and a galactosylated chitosan (galCHI) are employed. The latter choice is motivated by studies showing hepatocytes to bind specifically to galactose moieties [43,46]. As polypeptides, poly(L-lysine) (PLL) and poly(L-glutamic

acid) (PGA) are employed. The PLL-PGA system has been quite extensively studied: chondrosarcoma cells have been shown to adhere to PLL terminated films more strongly than to glass or PGA terminated films [20], and there is evidence of biocompatibility with SaOS-2 osteoblast-like cells for films ending with either PLL or PGA and with human periodontal ligament cells for films ending with PGA [47]. As synthetic polymers, poly(allylamine hydrochloride) (PAH) and poly(styrene sulfonate) (PSS) are employed. Previous work on this system has shown films ending by PAH to improve adhesion of endothelial cells compared to protein coatings [48], and films ending in PSS to support the attachment of primary hepatocytes from two month old rats [25,33]. We consider films formed from a single “class” of polymer, as well as those formed from a polysaccharide and a polypeptide. Moreover, we modify the mechanical rigidity of certain films through a chemical cross-linking protocol.

Hypothesizing that useful biomaterials must at a minimum support cell attachment and growth, we begin by screening a number of candidate multilayer films against a human liver cell line: HepG2. Next, we employ films upon which HepG2 reach confluence, and investigate the attachment, growth, and function of two primary cell systems: adult rat hepatocytes and human fetal hepatoblasts. In doing so, we seek both to identify best performing systems; to understand the role of film composition, rigidity, biofunctionality, and charge on liver cell behavior; and to compare outcomes between HepG2 and ARH, systems commonly used in basic research studies, and HFHb, representing a viable cell source for human transplantation. Below, we summarize our finding in terms of these key variables.

Film composition

We observe the type of polymers comprising the multilayer film biomaterial to play an important role in the cell response. As convincingly shown in Table 1, relatively few of the investigated polyelectrolyte pairs promote attachment and growth of the HepG2 cell line. Somewhat surprisingly, none of the pure polysaccharide films fared well, including those containing galactose units, previously shown to specifically enhance hepatocyte attachment [43,46]. While the $(PLL\text{-}ALG)_n$-PLL system promoted strong attachment in all three hepatocellular systems, attachment on $(PAH\text{-}PSS)_n$ by ARH was somewhat weaker than by HepG2 and HFHb, indicating a possible species specificity of this latter film. Film composition appears to play a large role in cell function as well: HFHb albumin production (in the absence of collagen) begins high and decreases about 30% over 8 days on the $(PLL\text{-}PGA)_n$-PLL film, begins low and increases 3 fold over 8 days on the $(PAH\text{-}PSS)_n$ film, and exhibits a mid-time point maximum on the $(PLL\text{-}ALG)_n$ film. The success of the PAH-PSS systems may be partially attributed to the known attraction between the side-chain styrene groups and hepatocytes [25,33]. It is tempting to partially attribute the success of PLL-PGA and PLL-ALG systems to the presence of PLL. Indeed, PLL is known to strongly complex with oppositely charged polymers, a feature contributing to film rigidity (see below). However, based on the present study, it is difficult to definitively explain why the PLL-containing systems promote liver cell attachment and growth to a far greater extent than do other seemingly comparable systems.

Film terminal layer

Film terminal layer strongly influences the attachment and growth of HepG2 and, for certain systems, HFHb. In the case of HepG2, the two films observed to promote confluent layers, $(PAH\text{-}PSS)_n$ and $(PLL\text{-}ALG)_n$-PLL-X, promote only sparse attachment when terminated with the opposite layer. Confluence is observed for HFHb i) on PLL-ALG films irrespective of terminal layer, ii) on PSS but not PAH terminated PAH-PSS films, iii) on PLL-PGA films irrespective of terminal layer in the presence of collagen, and iv) on PLL but not PGA terminated films in the absence of collagen. In contrast, film terminal layer appears to have little influence on the attachment of ARH.

Film rigidity

While the importance of surface chemistry on the behavior of contacting cells has long been considered, the importance of mechanical properties has only been recognized more recently. In particular, cell behavior has been shown to depend sensitively on multilayer film rigidity: osteoblasts showed increased long term proliferation [28], smooth muscle cells showed increased spreading [44], and chondrosarcoma cells showed increased attachment [23] on more rigid films. In this study, we seek to control film rigidity via EDC-NHS chemical cross-linking. We show, for the $(PLL\text{-}ALG)_n$-PLL system, HepG2 attachment and growth to be significantly enhanced by chemical cross-linking. However, no other system was positively affected in this way, including some films exhibiting appreciable HepG2 attachment/growth in the absence of cross-linking. In addition, it should be noted that the PAH-PSS system induces a comparable cell response to that of the cross-linked PLL-PGA and PLL-ALG systems, despite being significantly less rigid (in terms of QCMD measured mechanical moduli). Thus, factors beyond film rigidity are clearly at play here.

Film biofunctionality

Overall, we observe the presence of biofunctional species (collagen I and IV) on top of the multilayer film biomaterial to influence the behavior of hepatocellular systems in only certain cases. For example, the presence of collagen is critical in promoting ARH attachment for all but one film considered. In contrast, collagen plays a significant role in promoting HFHb attachment in only two systems: confluence is reached in the presence of either rCI and hCIV on $(PAH\text{-}PSS)_n$-PAH films at day 4 (but is not maintained through day 8), and confluence is maintained through day 8 in the presence of hCIV (but not rCI) in the $(PLL\text{-}PGA)_n$-X system. These observations point to a species-specific difference in the role of adsorbed collagen on the biomaterial-cell interaction. Collagen influences the albumin production of HFHb for the PLL-PGA and PLL-ALG, but not the PAH-PSS, systems. Interestingly, collagen can inhibit albumin production at short times (PLL-PGA system), but generally enhances albumin production at longer times. It is possible that the degree of conformational change among adsorbed collagen molecules differs among the systems investigated here, and that these differences are partially behind our observed system-dependent collagen effect.

Film charge

Overall film charge appears to be the least important variable for predicting cell behavior. For example, in the case of HepG2, of the two systems promoting significant cell attachment, one is positive and the other negative.

It is interesting to consider whether other film properties may play important roles in hepatocellular behavior. For example, film hydrophobicity is expected to vary among the systems considered here, with the general trend that chemical cross-linking [49] and protein adsorption [50] render hydrophilic surfaces (such as native polyelectrolyte multilayer films) more hydrophobic. Generally, cell attachment is weaker on more hydrophobic surfaces [51, 52], although the direct influence of hydrophobicity is difficult to distinguish from related properties, such as charge and tendency to adsorb protein [53]. Within this framework, our finding that chemical cross-linking enhances cell attachment and growth seems to suggest increased film rigidity to more than offset any increased hydrophobicity. At the same time, our finding that collagen has a fairly modest influence on cell attachment and growth may suggest increased hydrophobicity to partially offset the presence of biofunctional species.

Through these studies, we identify multilayer biomaterial systems upon which HFHb systems reach confluence within a few days. A common requirement being a large number of transplanted cells, these systems become top candidates for various liver tissue engineering applications. Among systems promoting confluent HFHb layers, $(PAH\text{-}PSS)_n$ is appealing

owing to its insensitivity to collagen and its promotion of a steadily increasing albumin secretion, a signal of healthy and functioning cells. Cross-linked $(PLL\text{-}ALG)_n$ and $(PLL\text{-}PGA)_n$-PLL also appear to be promising, in part owing to their expected biodegradability

5. Conclusion

We investigate here the attachment, growth, and function of rodent and human hepatocellular systems on multilayer nanofilm biomaterials formed via LbL assembly. We find film (polymer) composition, terminal layer, and rigidity to be the most important properties in promoting cell attachment, growth, and function. The influence of adsorbed proteins collagen I and IV is less pronounced, but some films perform better in the presence of these proteins. The direct influence of layer charge appears to be quite weak. Additionally, we observe important differences in the biomaterial-cell interaction due to cell age, immortalization state, and species. Through these studies, we identify the following nanofilm biomaterials as optimal in promoting confluent layers of functional cells within the HFHb system: $(PAH\text{-}PSS)_n$, cross-linked $(PLL\text{-}ALG)_n$, and cross-linked $(PLL\text{-}PGA)_n$-PLL. These systems become top candidates for *in vivo* human liver tissue engineering applications.

Acknowledgements

We are grateful to Jean Wilson for assistance with the albumin ELISA analysis, Kathy Harry and the Yale Liver Center (#DK-P30-34989) for providing adult rat hepatocytes, and the National Institutes of Health for financial support (through grant R01-EB00258).

References

1. Kulig KM, Vacanti JR. Hepatic tissue engineering. Transplant Immunology 2004;12(3–4):303–310. [PubMed: 15157923]
2. Cima LG, Vacanti JP, Vacanti C, Ingber D, Mooney D, Langer R. Tissue Engineering by Cell Transplantation Using Degradable Polymer Substrates. Journal of Biomechanical Engineering-Transactions of the ASME 1991;113(2):143–151.
3. Davis MW, Vacanti JP. Toward development of an implantable tissue engineered liver. Biomaterials 1996;17(3):365–372. [PubMed: 8745334]
4. Allen JW, Bhatia SN. Engineering liver therapies for the future. Tissue Engineering 2002;8(5):725–737. [PubMed: 12459052]
5. Chan C, Berthiaume F, Nath BD, Tilles AW, Toner M, Yarmush ML. Hepatic tissue engineering for adjunct and temporary liver support: Critical technologies. Liver Transplantation 2004;10(11):1331–1342. [PubMed: 15497161]
6. Hammond JS, Beckingham IJ, Shakesheff KM. Scaffolds for liver tissue engineering. Expert Review of Medical Devices 2006;3(1):21–27. [PubMed: 16359250]
7. Cima LG, Ingber DE, Vacanti JP, Langer R. Hepatocyte Culture on Biodegradable Polymeric Substrates. Biotechnology and Bioengineering 1991;38(2):145–158. [PubMed: 18600745]
8. Mooney D, Hansen L, Vacanti J, Langer R, Farmer S, Ingber D. Switching from Differentiation to Growth in Hepatocytes - Control by Extracellular-Matrix. Journal of Cellular Physiology 1992;151(3):497–505. [PubMed: 1295898]
9. Berthiaume F, Moghe PV, Toner M, Yarmush ML. Effect of extracellular matrix topology on cell structure, function, and physiological responsiveness: Hepatocytes cultured in a sandwich configuration. FASEB Journal 1996;10(13):1471–1481. [PubMed: 8940293]
10. Semler EJ, Ranucci CS, Moghe PV. Mechanochemical manipulation of hepatocyte aggregation can selectively induce or repress liver-specific function. Biotechnology and Bioengineering 2000;69(4):359–369. [PubMed: 10862674]
11. Semler EJ, Moghe PV. Engineering hepatocyte functional fate through growth factor dynamics: The role of cell morphologic priming. Biotechnology and Bioengineering 2001;75(5):510–520. [PubMed: 11745126]

12. Semler EJ, Lancin PA, Dasgupta A, Moghe PV. Engineering hepatocellular morphogenesis and function via ligand-presenting hydrogels with graded mechanical compliance. Biotechnology and Bioengineering 2005;89(3):296–307. [PubMed: 15744840]
13. Kamiya A, Kinoshita T, Ito Y, Matsui T, Morikawa Y, Senba E, et al. Fetal liver development requires a paracrine action of oncostatin M through the gp130 signal transducer. EMBO Journal 1999;18(8): 2127–2136. [PubMed: 10205167]
14. Kinoshita T, Sekiguchi T, Xu MJ, Ito Y, Kamiya A, Tsuji KI, et al. Hepatic differentiation induced by oncostatin M attenuates fetal liver hematopoiesis. Proceedings of the National Academy of Sciences of the United States of America 1999;96(13):7265–7270. [PubMed: 10377403]
15. Kamiya A, Kinoshita T, Miyajima A. Oncostatin M and hepatocyte growth factor induce hepatic maturation via distinct signaling pathways. FEBS Letters 2001;492(1–2):90−+. [PubMed: 11248243]
16. Kamiya A, Kojima N, Kinoshita T, Sakai Y, Miyaijma A. Maturation of fetal hepatocytes in vitro by extracellular matrices and oncostatin M: Induction of tryptophan oxygenase. Hepatology 2002;35 (6):1351–1359. [PubMed: 12029620]
17. Lazaro CA, Croager EJ, Mitchell C, Campbell JS, Yu CP, Foraker J, et al. Establishment, characterization, and long-term maintenance of cultures of human fetal hepatocytes. Hepatology 2003;38(5):1095–1106. [PubMed: 14578848]
18. Deurholt T, ten Bloemendaal L, Chhatta AA, van Wijk A, Weijer K, Seppen J, et al. In vitro functionality of human fetal liver cells and clonal derivatives under proliferative conditions. Cell Transplantation 2006;15(8–9):811–822. [PubMed: 17269451]
19. Dan YY, Riehle KJ, Lazaro C, Teoh N, Haque J, Campbell JS, et al. Isolation of multipotent progenitor cells from human fetal liver capable of differentiating into liver and mesenchymal lineages. Proceedings of the National Academy of Sciences of the United States of America 2006;103(26): 9912–9917. [PubMed: 16782807]
20. Richert L, Lavalle P, Vautier D, Senger B, Stoltz JF, Schaaf P, et al. Cell interactions with polyelectrolyte multilayer films. Biomacromolecules 2002;3(6):1170–1178. [PubMed: 12425653]
21. Mendelsohn JD, Yang SY, Hiller J, Hochbaum AI, Rubner MF. Rational design of cytophilic and cytophobic polyelectrolyte multilayer thin films. Biomacromolecules 2003;4(1):96–106. [PubMed: 12523853]
22. Jessel N, Atalar F, Lavalle P, Mutterer J, Decher G, Schaaf P, et al. Bioactive coatings based on a polyelectrolyte multilayer architecture functionalized by embedded proteins. Adv Mater 2003;15(9): 692–695.
23. Richert L, Boulmedais F, Lavalle P, Mutterer J, Ferreux E, Decher G, et al. Improvement of stability and cell adhesion properties of polyelectrolyte multilayer films by chemical cross-linking. Biomacromolecules 2004;5(2):284–294. [PubMed: 15002986]
24. Berg MC, Yang SY, Hammond PT, Rubner MF. Controlling mammalian cell interactions on patterned polyelectrolyte multilayer surfaces. Langmuir 2004;20(4):1362–1368. [PubMed: 15803720]
25. Kidambi S, Lee I, Chan C. Controlling primary hepatocyte adhesion and spreading on protein-free polyelectrolyte multilayer films. Journal of the American Chemical Society 2004;126(50):16286–16287. [PubMed: 15600306]
26. Tan W, Desai TA. Microscale multilayer cocultures for biomimetic blood vessels. Journal of Biomedical Materials Research Part A 2005;72A(2):146–160. [PubMed: 15558555]
27. Salloum DS, Olenych SG, Keller TCS, Schlenoff JB. Vascular smooth muscle cells on polyelectrolyte multilayers: Hydrophobicity-directed adhesion and growth. Biomacromolecules 2005;6(1):161–167. [PubMed: 15638516]
28. Picart C, Elkaim R, Richert L, Audoin T, Arntz Y, Cardoso MD, et al. Primary cell adhesion on RGD-functionalized and covalently crosslinked thin polyelectrolyte multilayer films. Advanced Functional Materials 2005;15(1):83–94.
29. Benkirane-Jessel N, Lavalle P, Hubsch E, Holl V, Senger B, Haikel Y, et al. Short-time timing of the biological activity of functionalized polyelectrolyte multilayers. Advanced Functional Materials 2005;15(4):648–654.
30. Kreke MR, Badami AS, Brady JB, Akers RM, Goldsteinx AS. Modulation of protein adsorption and cell adhesion by poly(allylamine hydrochloride) heparin films. Biomaterials 2005;26(16):2975–2981. [PubMed: 15603792]

31. Jessel N, Oulad-Abdeighani M, Meyer F, Lavalle P, Haikel Y, Schaaf P, et al. Multiple and time-scheduled in situ DNA delivery mediated by beta-cyclodextrin embedded in a polyelectrolyte multilayer. Proceedings of the National Academy of Sciences of the United States of America 2006;103(23):8618–8621. [PubMed: 16735471]
32. Wittmer CR, Phelps JA, Saltzman WM, Van Tassel PR. Fibronectin terminated multilayer films: Protein adsorption and cell attachment studies. Biomaterials 2007;28(5):851–860. [PubMed: 17056106]
33. Kidambi S, Sheng LF, Yarmush ML, Toner M, Lee I, Chan C. Patterned co-culture of primary hepatocytes and fibroblasts using polyelectrolyte multilayer templates. Macromolecular Bioscience 2007;7(3):344–353. [PubMed: 17370273]
34. Nellen PM, Tiefenthaler K, Lukosz W. Integrated Optical Input Grating Couplers as Biochemical Sensors. Sensors and Actuators 1988;15(3):285–295.
35. Lukosz W, Clerc D, Nellen PM, Stamm C, Weiss P. Output Grating Couplers on Planar Optical Wave-Guides as Direct Immunosensors. Biosens Bioelectron 1991;6(3):227–232. [PubMed: 1883602]
36. Ramsden JJ. Review of New Experimental-Techniques for Investigating Random Sequential Adsorption. J Stat Phys 1993;73(5–6):853–877.
37. Voros J, Ramsden JJ, Csucs G, Szendro I, De Paul SM, Textor M, et al. Optical grating coupler biosensors. Biomaterials 2002;23(17):3699–3710. [PubMed: 12109695]
38. Tiefenthaler K, Lukosz W. Sensitivity of Grating Couplers as Integrated-Optical Chemical Sensors. J Opt Soc Am B-Opt Phys 1989;6(2):209–220.
39. Rodahl M, Hook F, Krozer A, Brzezinski P, Kasemo B. Quartz-Crystal Microbalance Setup for Frequency and Q-Factor Measurements in Gaseous and Liquid Environments. Review of Scientific Instruments 1995;66(7):3924–3930.
40. Rodahl M, Kasemo B. Frequency and dissipation-factor responses to localized liquid deposits on a QCM electrode. Sensors and Actuators B-Chemical 1996;37(1–2):111–116.
41. Rodahl M, Hook F, Kasemo B. QCM operation in liquids: An explanation of measured variations in frequency and Q factor with liquid conductivity. Analytical Chemistry 1996;68(13):2219–2227.
42. Rodahl M, Hook F, Fredriksson C, Keller CA, Krozer A, Brzezinski P, et al. Simultaneous frequency and dissipation factor QCM measurements of biomolecular adsorption and cell adhesion. Faraday Discussions 1997;(107):229–246. [PubMed: 9569776]
43. Chung TW, Yang J, Akaike T, Cho KY, Nah JW, Kim SI, et al. Preparation of alginate/galactosylated chitosan scaffold for hepatocyte attachment. Biomaterials 2002;23(14):2827–2834. [PubMed: 12069321]
44. Richert L, Engler AJ, Discher DE, Picart C. Elasticity of native and cross-linked polyelectrolyte multilayer films. Biomacromolecules 2004;5(5):1908–1916. [PubMed: 15360305]
45. Boyer JL, Phillips JM, Graf J. Preparation and Specific Applications of Isolated Hepatocyte Couplets. Methods in Enzymology 1990;192:501–516. [PubMed: 1963665]
46. Park IK, Yang J, Jeong HJ, Bom HS, Harada I, Akaike T, et al. Galactosylated chitosan as a synthetic extracellular matrix for hepatocytes attachment. Biomaterials 2003;24(13):2331–2337. [PubMed: 12699671]
47. Tryoen-Toth P, Vautier D, Haikel Y, Voegel JC, Schaaf P, Chluba J, et al. Viability, adhesion, and bone phenotype of osteoblast-like cells on polyelectrolyte multilayer films. Journal of Biomedical Materials Research 2002;60(4):657–667. [PubMed: 11948525]
48. Boura C, Menu P, Payan E, Picart C, Voegel JC, Muller S, et al. Endothelial cells grown on thin polyelectrolyte mutlilayered films: an evaluation of a new versatile surface modification. Biomaterials 2003;24(20):3521–3530. [PubMed: 12809781]
49. Khopade AJ, Caruso F. Surface-modification of polyelectrolyte multilayer-coated particles for biological applications. Langmuir 2003;19(15):6219–6225.
50. Horbett TA. Principles Underlying the Role of Adsorbed Plasma-Proteins in Blood Interactions with Foreign Materials. Cardiovascular Pathology 1993;2(3):S137–S148.
51. Vogler EA. Structure and reactivity of water at biomaterial surfaces. Advances in Colloid and Interface Science 1998;74:69–117. [PubMed: 9561719]
52. Ma ZW, Mao ZW, Gao CY. Surface modification and property analysis of biomedical polymers used for tissue engineering. Colloids and Surfaces B-Biointerfaces 2007;60(2):137–157.

53. Wilson CJ, Clegg RE, Leavesley DI, Pearcy MJ. Mediation of biomaterial-cell interactions by adsorbed proteins: A review. Tissue Engineering 2005;11(1–2):1–18. [PubMed: 15738657]

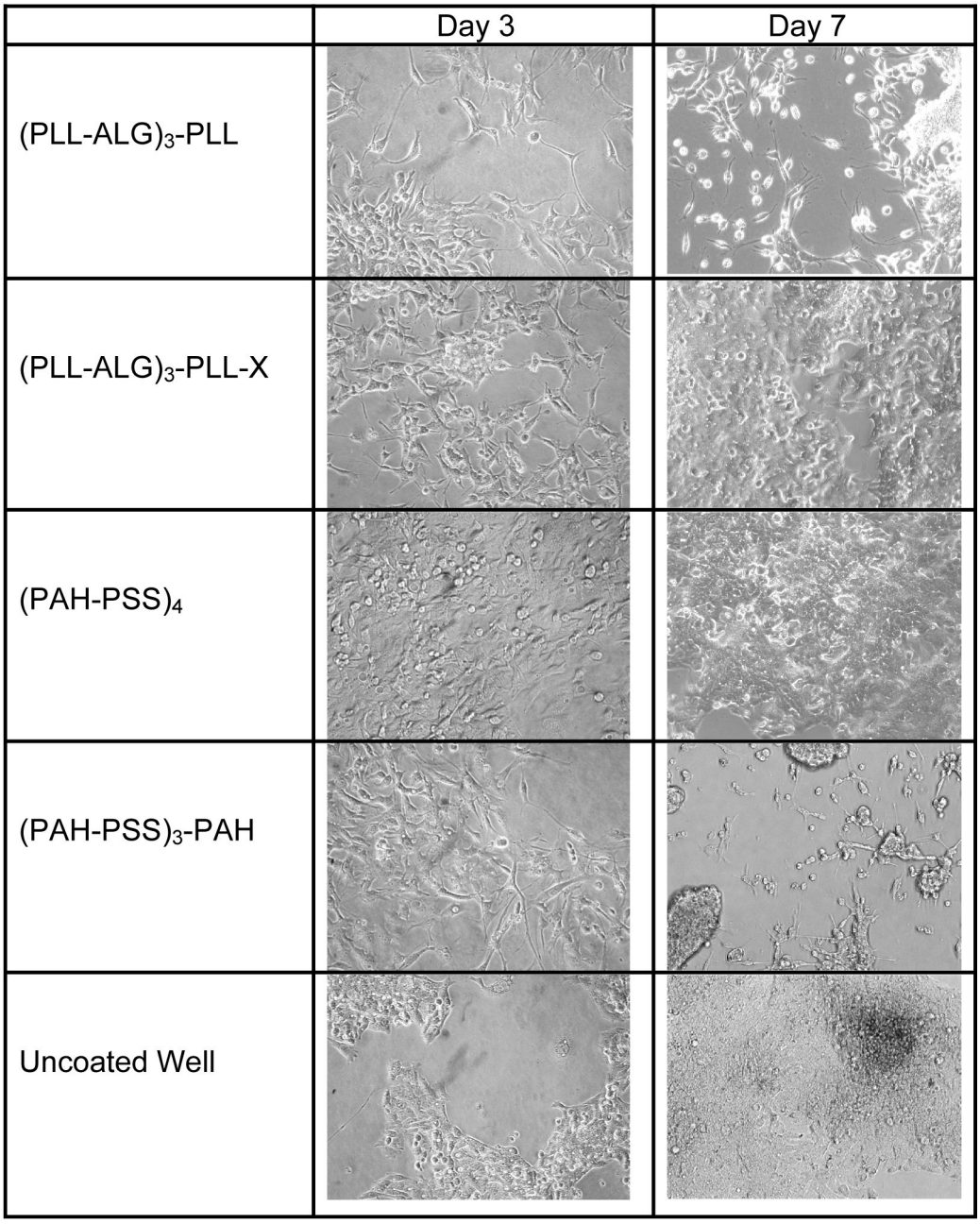

Fig. 1.

Photomicrographs of HepG2 taken after 3 and 7 days culture on $(PLL\text{-}ALG)_3$-PLL, $(PLL\text{-}ALG)_3$-PLL-X, $(PAH\text{-}PSS)_4$, $(PAH\text{-}PSS)_3$-PAH, and the uncoated culture well.

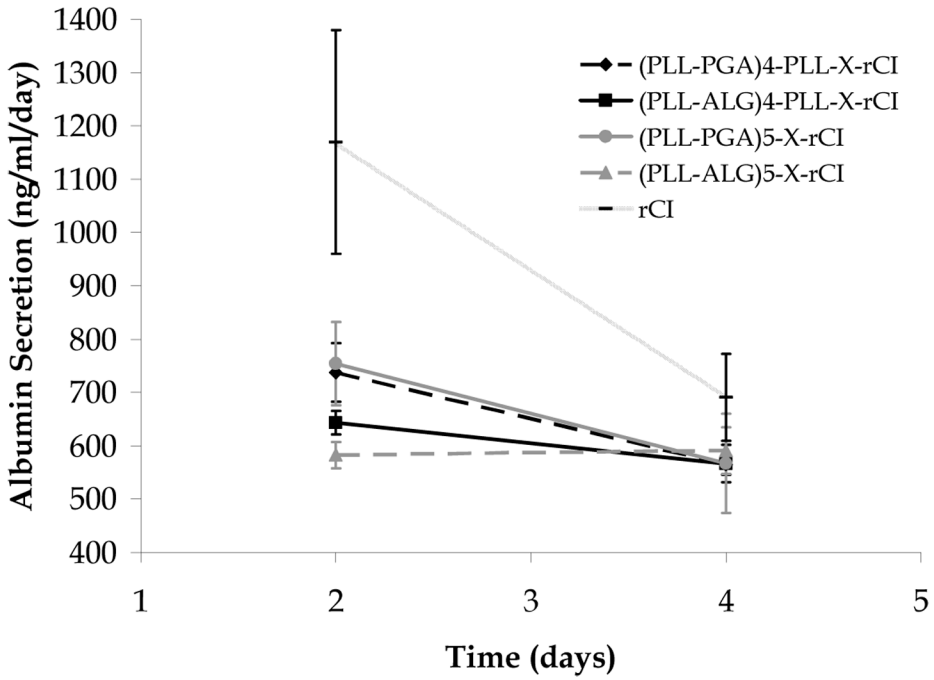

Fig. 2.
Albumin secretion rate for ARH seeded on various multilayer films and on a rat collagen I coated plate (Biocoat).

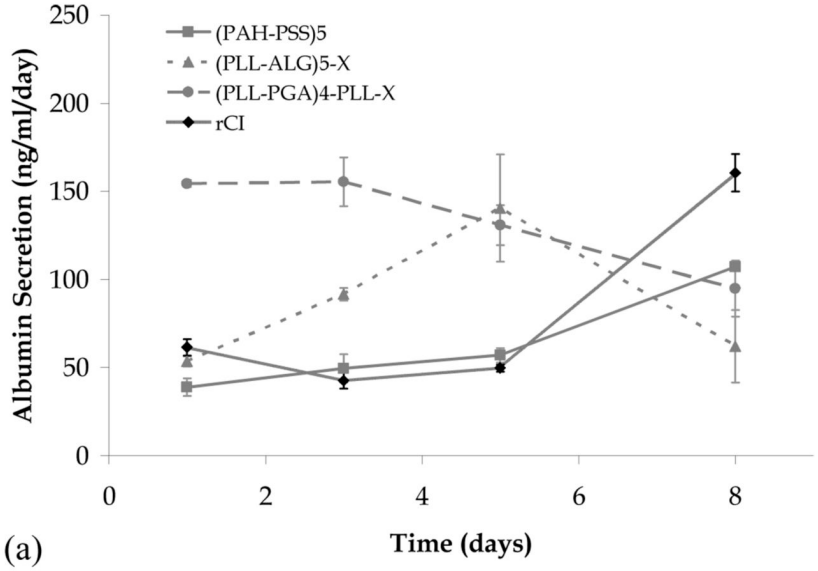

(a)

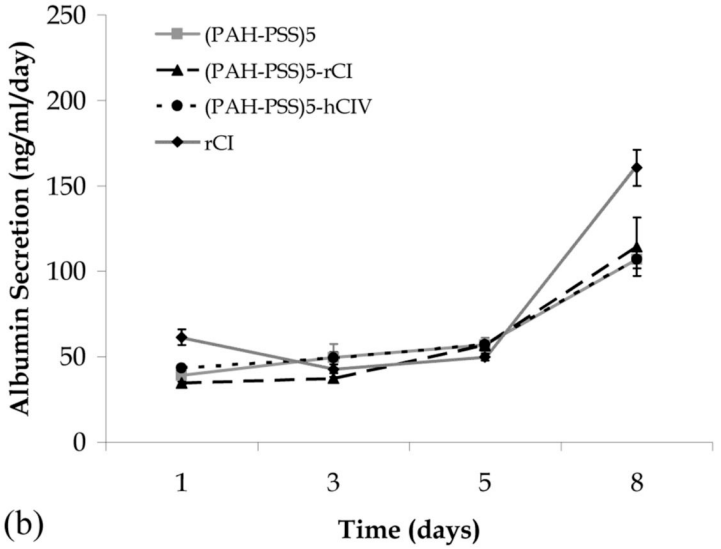

(b)

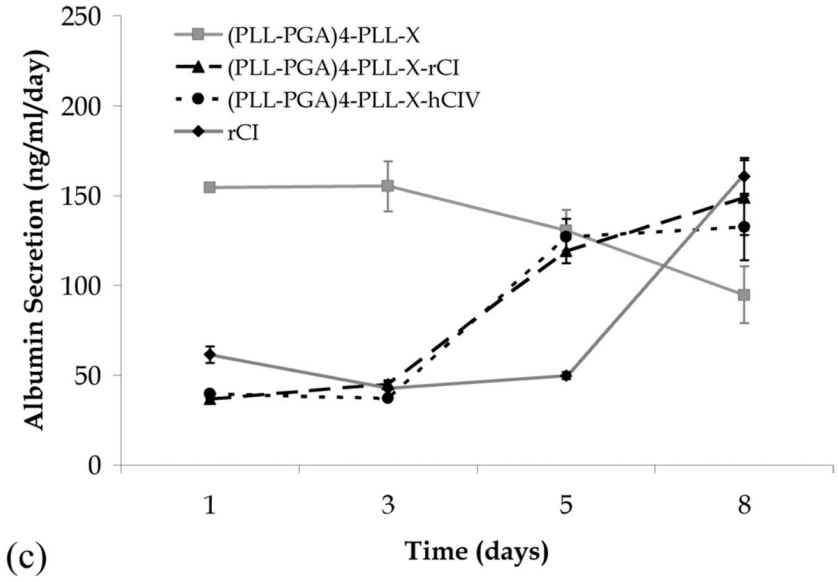

(c)

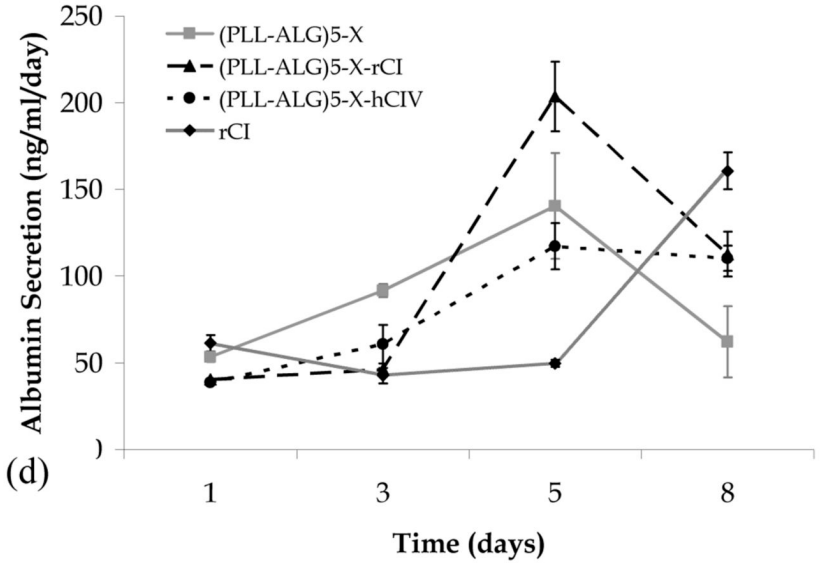

(d)

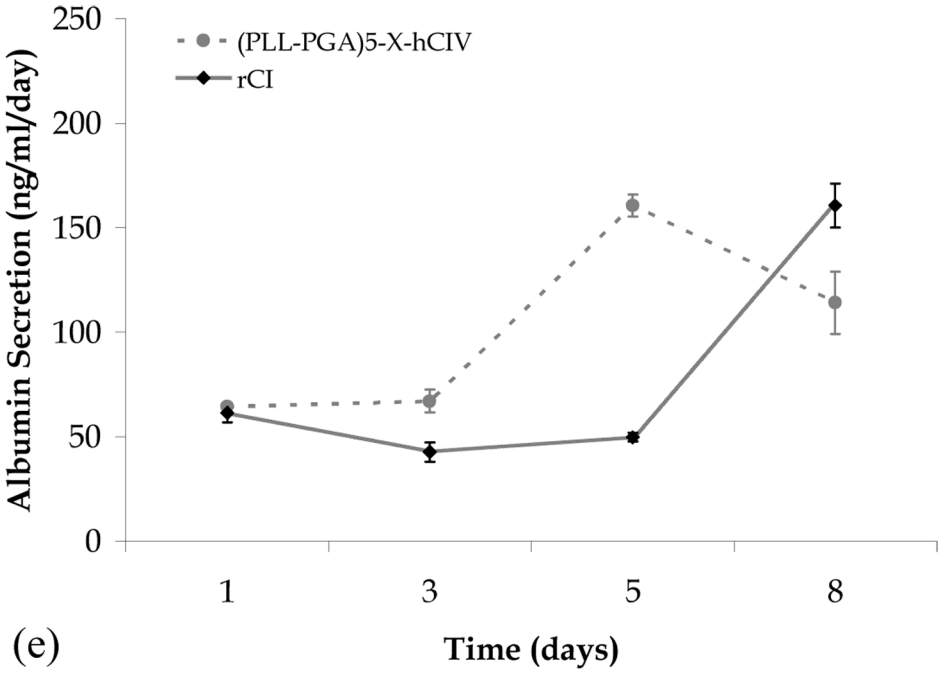

Fig. 3.

Albumin secretion versus time for human fetal hepatoblasts seeded on various multilayer film biomaterials. (a) confluent systems in the absence of collagen, (b) PAH-PSS systems, (c) PLL-PGA systems, (d) PLL-ALG systems, and (e) confluent systems in the presence of collagen not shown in (b)–(d).

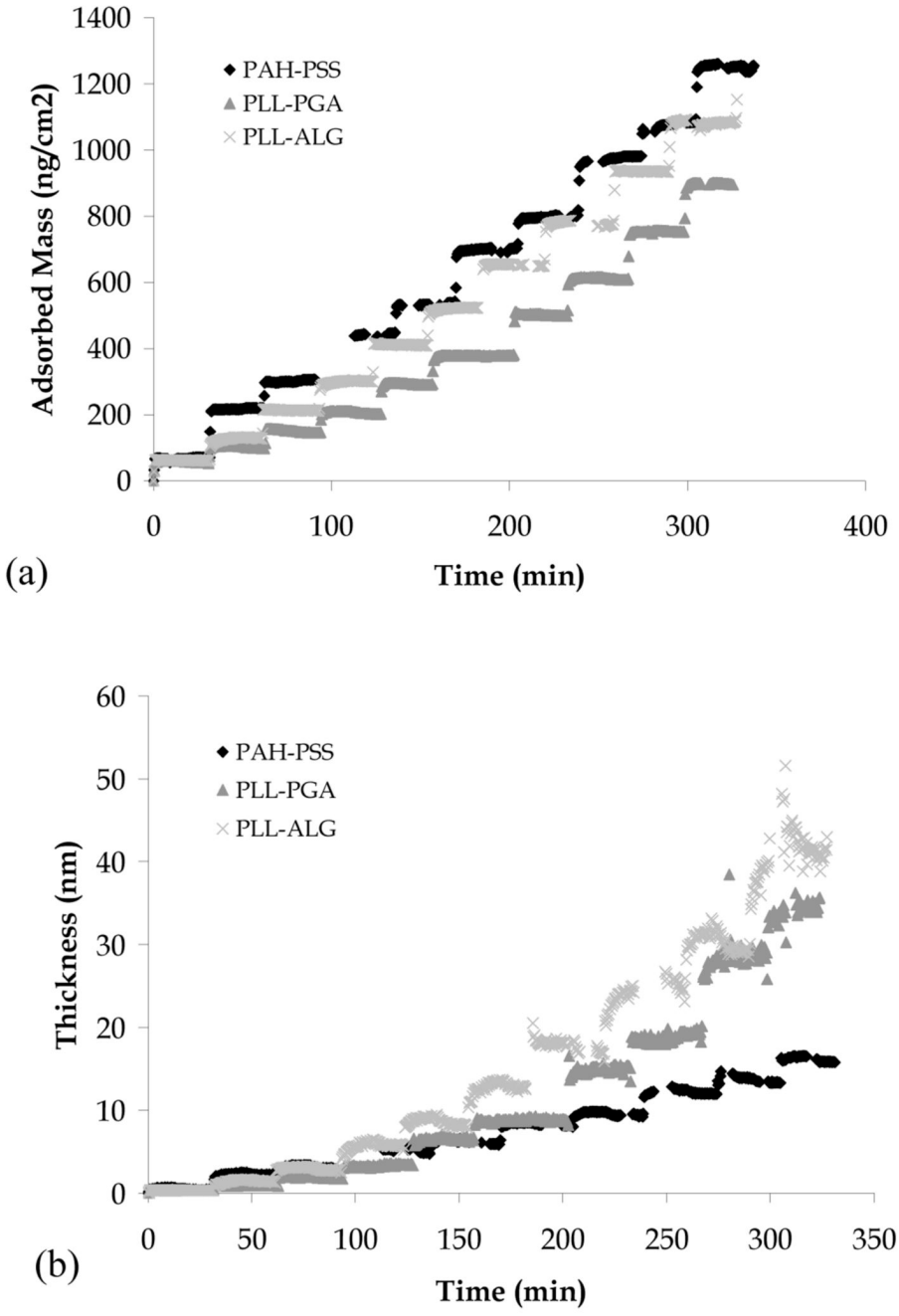

Fig. 4.
Mass (a) and thickness (b) of PAH-PSS, PLL-ALG, and PLL-PGA films during LbL assembly, as measured by OWLS.

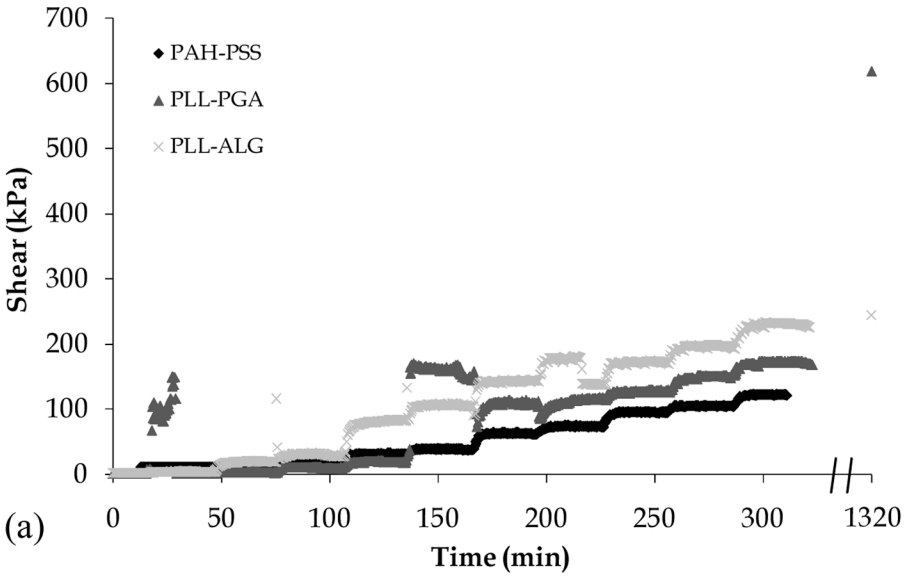

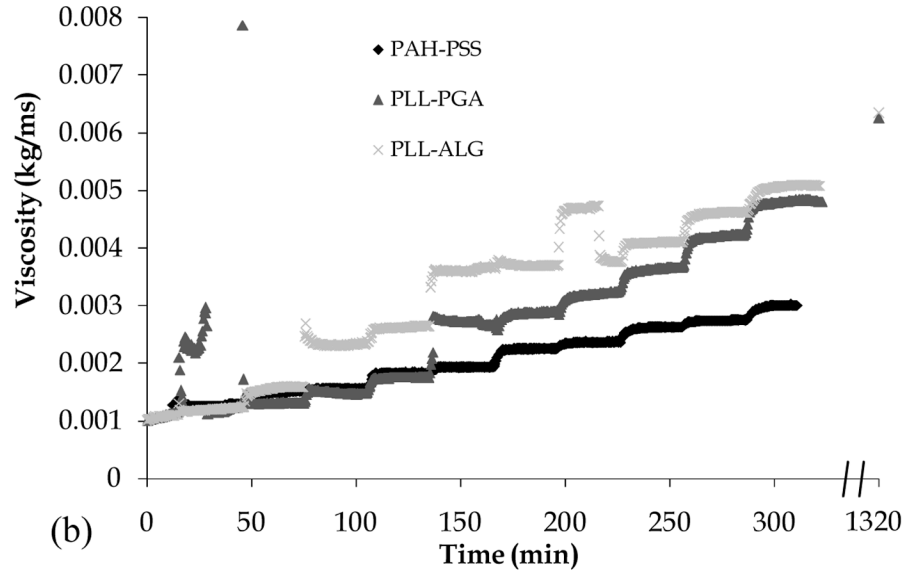

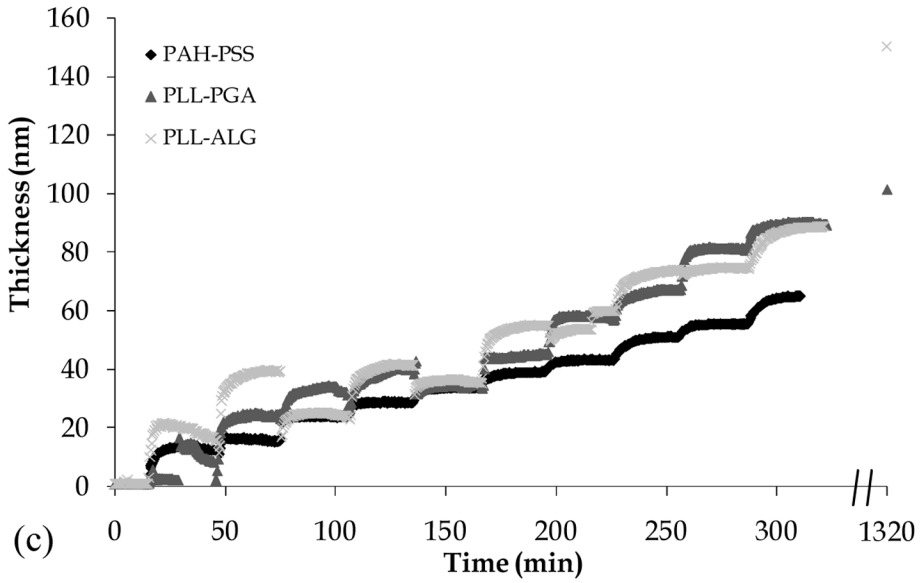

Fig. 5.

Shear modulus (a), viscosity (b), and thickness (c) of PAH-PSS, PLL-ALG, and PLL-PGA films during LbL assembly, as measured by QCMD. Data points along right vertical axis are taken following film exposure to chemical cross-linking agents (see Section 2.3).

Table 1

The percent coverage of HepG2 cells seeded onto various multilayer films, as determined by phase contrast micrographs taken at 3 and 7 days in culture. Lack of data implies negligible cell attachment. The bare tissue culture polystyrene well serves as the control.

Type of Film	Film Composition	% Coverage Day 3	% Coverage Day 7
Synthetic	$(PAH\text{-}PSS)_4$	100 %	100%
	$(PAH\text{-}PSS)_3$-PSS	70–80%	10–20%
Polysaccharide	$(CHI\text{-}ALG)_4$	---	---
	$(CHI\text{-}ALG)_3$-CHI	---	---
	$(GALCHI\text{-}ALG)_4$	---	---
	$(GALCHI\text{-}ALG)_3$-galCHI	---	---
Polysaccharide-Polypeptide	$(CHI\text{-}PGA)_4$	---	---
	$(CHI\text{-}PGA)_3$-CHI	10–20%	---
	$(PLL\text{-}ALG)_4$	5–10%	10–20%
	$(PLL\text{-}ALG)_3$-PLL	30–40%	20–30%
Cross-Linked Polysaccharide	$(CHI\text{-}ALG)_4$-X	---	---
	$(CHI\text{-}ALG)_3$-CHI-X	---	---
	$(GALCHI\text{-}ALG)_4$-X	---	---
	$(GALCHI\text{-}ALG)_3$-GALCHI-X	---	---
Cross-linked Polysaccharide- Polypeptide	$(CHI\text{-}PGA)_4$-X	---	---
	$(CHI\text{-}PGA)_3$-CHI-X	10–20%	---
	$(PLL\text{-}ALG)_4$-X	---	---
	$(PLL\text{-}ALG)_3$-PLL-X	70–80%	100%
No film (Control)	---	30–40%	100%

Table 2

The percent coverage of primary (passage 0) adult rat hepatocytes (ARH) seeded onto various multilayer films, as determined by phase contrast micrographs taken at 1 and 3 days in culture. Lack of data implies negligible cell attachment. A rat collagen I (rCI) coated well (Biocoat) serves as the control.

Type of Film	Film Composition	% Coverage Day 1	% Coverage Day 3
Synthetic	$(PAH\text{-}PSS)_5$	20–30%	20–30%
	$(PAH\text{-}PSS)_5$-rCI	30–40%	20–30%
	$(PAH\text{-}PSS)_4$-PAH	---	---
	$(PAH\text{-}PSS)_4$-PAH-rCI	30–40%	20–30%
Polysaccharide-Polypeptide	$(PLL\text{-}ALG)_5$-X	---	---
	$(PLL\text{-}ALG)_5$-X-rCI	70–80%	60–70%
	$(PLL\text{-}ALG)_4$-PLL-X	---	---
	$(PLL\text{-}ALG)_4$-PLL-X-rCI	60–70%	60–70%
Polypeptide	$(PLL\text{-}PGA)_5$-X	40–50%	---
	$(PLL\text{-}PGA)_5$-X-rCI	60–70%	40–50%
	$(PLL\text{-}PGA)_4$-PLL-X	40–50%	---
	$(PLL\text{-}PGA)_4$-PLL-X-rCI	70–80%	60–70%
Control	rCI	70–80%	60–70%

Table 3

The percent coverage of passage 1 human fetal hepatoblasts (HFHb) and associated stromal cells -- harvested from rat collagen I adsorbed flasks using EGTA/collagenase-dispase -- seeded onto various multilayer films, as determined by phase contrast micrographs taken at 1, 4, and 8 days in culture. Lack of data implies negligible cell attachment. A rat collagen I (rCI) coated well (Biocoat) serves as the control.

Multilayer Film	Day 1	Day 4	Day 8
$(PAH\text{-}PSS)_5$	98%	100%	100%
$(PAH\text{-}PSS)_5$-rCI	90%	100%	100%
$(PAH\text{-}PSS)_5$-hCIV	95%	100%	100%
$(PAH\text{-}PSS)_4$-PAH	5%	3%	0%
$(PAH\text{-}PSS)_4$-PAH-rCI	30%	95%*	1%
$(PAH\text{-}PSS)_4$-PAH-hCIV	40%	100%*	0%
$(PLL\text{-}ALG)_5$-X	100%	100%	100%
$(PLL\text{-}ALG)_5$-X-rCI	80%	98%	100%
$(PLL\text{-}ALG)_5$-X-hCIV	95%	100%	100%
$(PLL\text{-}ALG)_4$-PLL-X	10%	50%	98%
$(PLL\text{-}ALG)_4$-PLL-X-rCI	30%	50%	100%
$(PLL\text{-}ALG)_4$-PLL-X-hCIV	5%	30%	100%*
$(PLL\text{-}PGA)_5$-X	50%	95%	10%
$(PLL\text{-}PGA)_5$-X-rCI	80%	100%	2%
$(PLL\text{-}PGA)_5$-X-hCIV	95%	100%	100%
$(PLL\text{-}PGA)_4$-PLL-X	80%	100%	100%
$(PLL\text{-}PGA)_4$-PLL-X-rCI	70%	100%	100%
$(PLL\text{-}PGA)_4$-PLL-X-hCIV	90%	100%	100%
rCI	20%	30%	100%

* Contracting phenotype observed

Table 4

Mass and thickness of multilayer films before and after chemical cross-linking, and mass of human collagen I and IV adsorbed to PAH-PSS and cross-linked PLL-ALG and PLL-PGA films, as measured via OWLS. ST = bare silica-titania OWLS sensor chip.

	Before cross-linking		After cross-linking		hCI	hCIV
	Thickness (nm)	Mass (ng/cm^2)	Thickness (nm)	Mass (ng/cm^2)	Mass (ng/cm^2)	Mass (ng/cm^2)
ST					160 ± 10	260 ± 10
$(PLL\text{-}ALG)_5$	38 ± 3	1110 ± 20	27 ± 1	1280 ± 40	98 ± 3	19 ± 1
$(PLL\text{-}ALG)_4\text{-}PLL$	27 ± 2	920 ± 50	21 ± 1	1080 ± 70	27 ± 1	---
$(PLL\text{-}PGA)_5$	32 ± 3	920 ± 20	18 ± 1	1040 ± 30	70 ± 2	140 ± 4
$(PLL\text{-}PGA)_4\text{-}PLL$	25 ± 2	770 ± 30	14 ± 1	940 ± 20	55 ± 2	78 ± 2
$(PAH\text{-}PSS)_5$	16 ± 1	1290 ± 40			230 ± 10	390 ± 10
$(PAH\text{-}PSS)_4\text{-}PAH$	14 ± 1	1120 ± 30			160 ± 10	510 ± 20